LABORATORY MODELLING OF EROSION DAMAGE BY VORTICES IN SLURRY FLOW

L.J.W. Graham[1], J Wu[1], G. Short[1], C. Solnordal[1], C. Wong[1], G. Brown[2], O. Celliers[2] and D Whyte[2]

[1] *CSIRO Mineral Resources Flagship, Melbourne, Victoria, Australia*

[2] *Alcoa, Cockburn Road, Kwinana, WA, Australia*

Corresponding author: jie.wu@csiro.au

ABSTRACT

There are on-going maintenance costs and production losses due to particulate erosion damage in slurry flow equipment used in slurry transport and processing equipment in alumina refineries. CSIRO has been conducting research under AMIRA P931 "Multiphase Flow Erosion" projects since 2006, under sponsorship funding support from Alcoa, BHPB, Rio Tinto Alcan, Vale and Pentair Valves (Tyco Flow). AMIRA P931 projects focused on building knowledge and methods to predict the erosion service life of flow equipment and developing strategies through case studies to alter flow design to reduce erosion and extend equipment life. Interestingly, none of the case studies requested by the industry partners involved simple impingement erosion or sliding bed erosion. As the emphasis has been on solving erosion problems using the principles of the underlying multiphase fluid dynamics, this called for an in-depth CFD treatment of non-uniform flows. In this the current study was very different from the usual treatment of erosion, which focuses on direct impingement simply because it is easy to model and measure, and rather addressed the much more common industrial problem of localised erosion.

The importance of several fluid dynamic mechanisms responsible for severe erosion attacks was reinforced during the P931 projects with quantitative measurements of the details of the erosion being made available. These include erosion by vortices, by flashing and by various non-uniform flows. For example, erosion by vortices which tend to cause more damage than "normal flow" was found to be caused by the effect of multiple hits by solids trapped in the vortices compared with single hits by solids in a direct impact condition. This finding of accelerated wear has allowed the diagnosis of vortex erosion being present in many flow geometries critically important in P931 sponsors' plants, e.g. pipework around a valve, protrusions in a pipe and many conventional engineering designs. The present paper focuses on vortex erosion as noted in a variety of flow situations and examines the fluid dynamics and consequent erosion.

1. INTRODUCTION

Severe erosion attack can occur in mineral process plants where complex fluid dynamics occurs. Vortex flows are one example of this and have been discussed in the literature by (Brown 2002) in the context of a blanked tee in pipe work and (Graham et al. 2010) who examined the flow around obstacles and the consequent erosion. A good summary of the details of vortex flows caused by obstacles is given by (Simpson 2001).

A tee section is commonly encountered where the flow is required to be sent into one of two possible directions, where the unused flow path could, for example, be closed by a knife gate valve. Blanking plates are also used for more long term blockage of the unused leg. Under some circumstances it is known that a vortex can develop in the tee which leads to significant erosion on the blanking plate or valve blade ((Brown 1999) and (Brown 2002)). The generic flow geometry is shown in Figure 1.

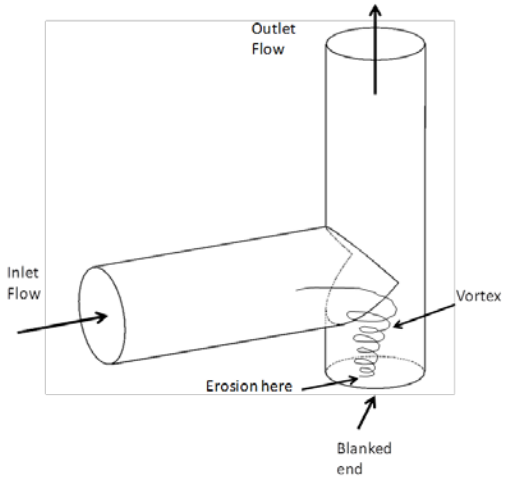

Figure 1. Generic blanked tee geometry. The blanked end may be due to a valve being closed for example

This flow has previously been the subject of a CFD study by (Brown 1999) and (Brown 2002). The CFD results in these papers

showed that a vortex was present at the position of the maximum erosion on the blanked end provided some swirl was present in the inlet flow. A photograph of a full scale eroded blanking plate is shown in Figure 2 (a) (from (Brown 2002)). No erosion modelling was presented in these papers, although paint was used to visualize the erosion pattern in laboratory at CSIRO (Figure 2 (b)).

(a)

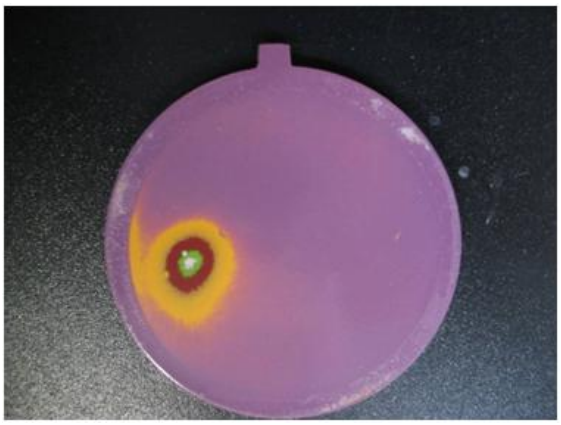

(b)

Figure 2. (a) Full scale example of erosion in tee blank, (Brown 2002), (b) paint erosion model from (Wu et al. 2011).

This paper presents examples of the erosion due to vortex action around obstacles and that due to a blanked tee.

2. EXPERIMENTAL METHODS

The erosion tests were conducted in a slurry rig with the schematic shown in Figure 3. The rig consists of a 3000L agitated tank, Warman 4x3 AH slurry pump, magnetic flowmeter and appropriate connecting pipe work in NB 50mm pipe. The sample is arranged in a straight, vertical length of pipe. Normally a straight length of pipe of at least 20 diameters is provided before the sample, and the rig can be configured for up to 4 samples simultaneously if required. Cylindrical samples of the same material as the sample under investigation are usually tested at the same time as a control sample undergoing direct impact erosion.

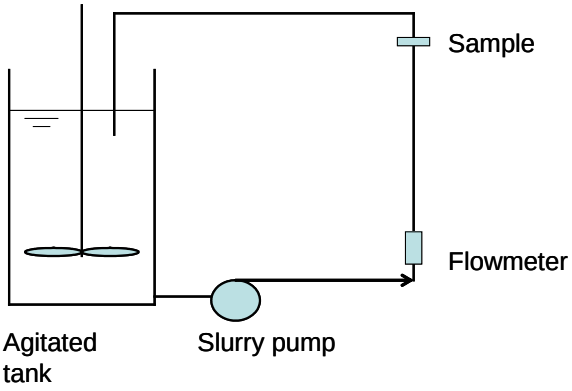

Figure 3. Schematic of pipe loop erosion test rig.

Figure 4. Photograph of CSIRO erosion rig

All erosion measurements were made using the Sheffield Discovery 11 coordinate measurement machine (CMM) as shown in Figure 5. The repeatability of measurements made using the CMM was of the order of 3 μm.

Figure 5. Sheffield Discovery II coordinate measurement machine (CMM) at CSIRO Fluids Engineering laboratory, 2011

2.1 Vortex erosion around an obstacle

A pipe with an obstacle in slurry flow was studied as shown in Figure 6. The pipe was made from two pieces of aluminium (6061-T6) with a 53 mm diameter section machined out of each piece. This allowed for access for the touch probe of the coordinate measurement machine (CMM). The obstacle was a 16 mm diameter cylindrical stainless steel pin inset into the pipe and protruding approximately half way across the pipe cross-section. Using stainless steel for the obstacle ensured that it did not erode significantly during the test programme. A replaceable plug contoured to the shape of the pipe wall was also made in order to allow for good access for the CMM probe as shown in Figure 7. A 1 mm CMM probe was used for all tests. Table 1 shows the nominal test conditions.

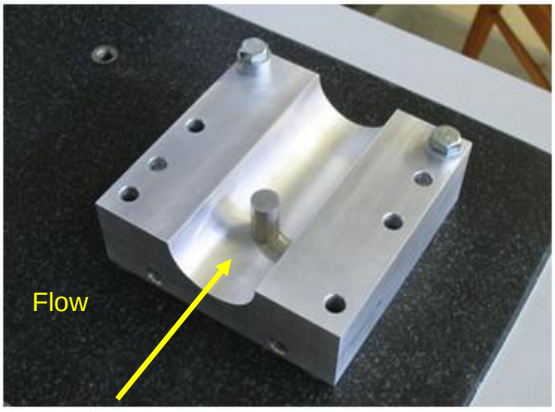

Figure 6. Pipe geometry with cylindrical obstacle, mounted on Coordinate Measurement Machine. Arrow indicates flow direction

Figure 7. Measuring the uneroded condition of the experimental test section. The obstacle has been removed and a plug has been inserted to allow for probe access in the immediate vicinity of the obstacle

Table 1. Test conditions.

Pipe	ID nominal 53 mm, 150 mm in length
Obstacle	OD 16 mm, height 26.5 mm
Material	Aluminium (for rapid tests)
Solids type	Unimin Silica Flour 100G
Solids d_{50}	25 µm approx
Fluid	Water
Solids C_v	12% (v/v)
Velocity	4.5 m s^{-1}

A cylinder sample of identical material (6061 –T6 aluminium) to the pipe piece was also

used for simultaneous cylinder-in-pipe tests, in the same flow at the same time. This allowed for a comparison between the direct impact type of erosion on the cylinder and that caused by the vortex. A schematic diagram of the cylinder-in-pipe test is shown in Figure 8. Further cylinder tests were performed at 3 and 6 m s^{-1} in order to provide calibration data for erosion modelling.

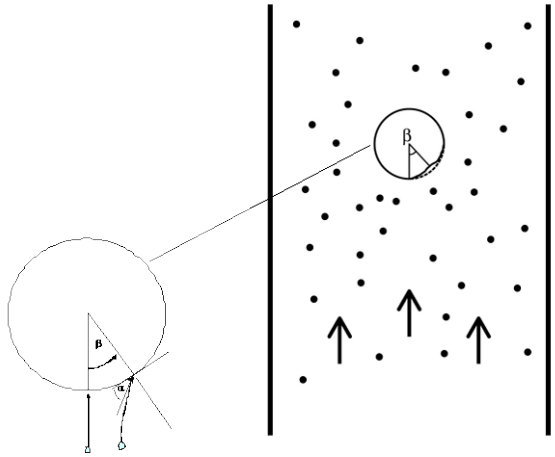

Figure 8. Schematic diagram of cylinder in pipe erosion calibration

Other obstacles were considered including cable ties around the reference cylinder and are discussed further in section 3.

2.2 Erosion due to vortex in a blanked tee

A tee rig was designed and manufactured from 316L stainless steel pipe. A schematic of the tee is shown in Figure 9 a swirler was incorporated into the rig as it was known from previous work ((Brown 2002)), that a degree of swirl was required in order to develop the vortex on the blanked end. The swirler was arranged such that the vanes turn 90° in 2 pipe diameters.

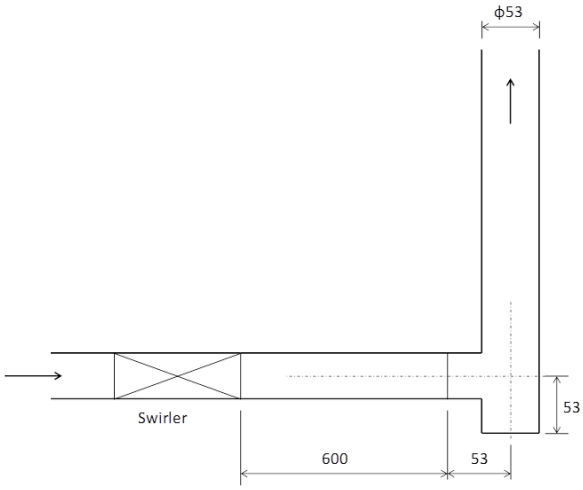

Figure 9. Tee schematic. Arrows indicate flow direction

It should be explained that experiments with the swirler removed showed that the vortex is naturally generated in the tee. The swirler was used here to “condition” the vortex so that the swirling velocity is more controlled with a stable boundary condition.

3. RESULTS AND DISCUSSION

3.1 Vortex erosion around an obstacle

It is known that vortex erosion occurs in plant situations and it would be desirable to have a ranking test for materials under the conditions of vortex erosion. The horseshoe vortex has the advantage of being readily reproducible and geometrically simple. It is thus a good candidate geometry for erosion tests.

Figure 10 shows the erosion obtained after 2 hours of exposure. It is seen that the maximum erosion is of the order of 0.11 mm and is close to the junction between the obstacle and the pipe wall. At the end of the tests, after 170 hours of exposure, the maximum erosion is of the order of 3.3 mm as shown in Figure 11. The 170 hours case also shows the formation of secondary erosion scars behind the first large erosion scar. These can also be seen in photographs of the erosion in Figure 12. It is a reasonable hypothesis that given the formation of a relatively deep initial erosion scar, the flow disturbance thus caused may cause a further erosion increase in the immediate vicinity of the scar.

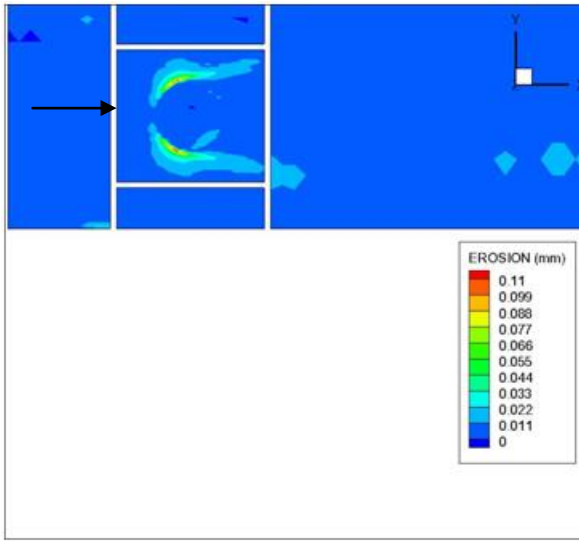

Figure 10. Measurement of erosion at 2 hours

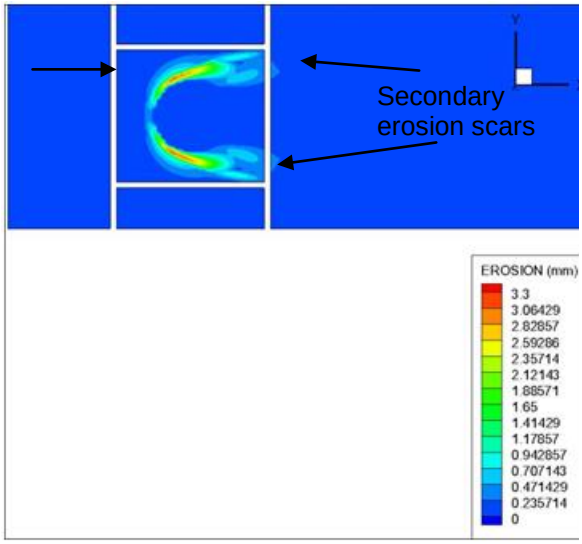

Figure 11. Measurement of erosion at 170 hours

It is considered that the erosion shown above is a consequence of vortex action. The CFD results (discussed below) show the existence of a horseshoe vortex around the obstacle which is expected for this kind of flow around a surface mounted obstacle.

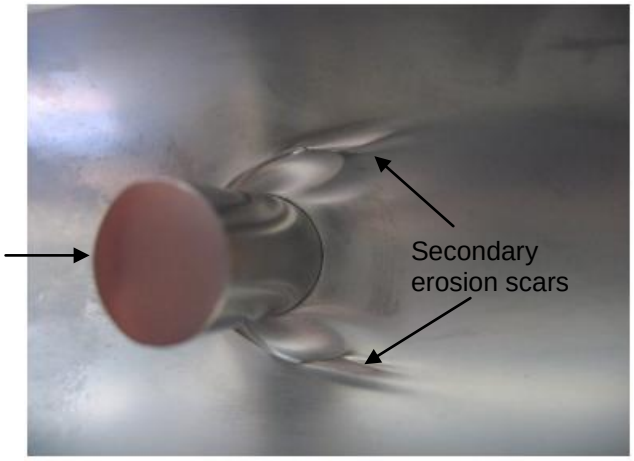

Figure 12. Photograph of the erosion at 170 hours exposure

The ratio between the erosion due to the vortex and that due to direct impact on the cylinder is shown in Figure 13. The ratio is approximately 3 after the initial erosion. Also shown is the ratio between the erosion due to the horseshoe vortex and the erosion on the pipe wall away from and unaffected by the horseshoe vortex. Of interest here is that the erosion due to the horseshoe vortex can be of the order of 80 times the erosion on the pipe wall itself.

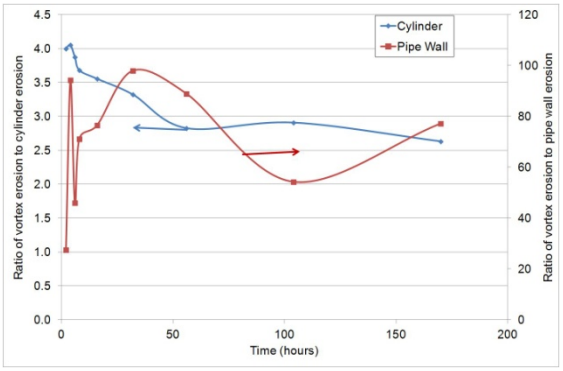

Figure 13. Blue line - ratio of maximum erosion due to vortex and the maximum erosion on the cylinder. Red line - ratio of the maximum erosion due to the vortex and the maximum erosion on the pipe wall away from the vortex

Computational Fluid Dynamics (CFD) results are presented in Figure 14 using the pristine geometry (time = 0 hr). Figure 14 shows a plan view of the velocity distribution around the obstacle at a distance of 0.5 mm from the pipe wall. The image shows the expected characteristics of flow around a cylinder. Specifically, a stagnation point exists

immediately upstream of the obstacle, water accelerates around the obstacle with velocities as high as 8 m s^{-1}, and there is a recirculation region behind the obstacle (where flow is expected to be unsteady).

Figure 15 shows a plot of the surface of constant swirl vector which shows the development of the horseshoe vortex around the obstacle. Thus far it is clear that the CFD can predict the vortex responsible for the accelerated erosion but quantitative erosion rate prediction from the CFD model is still a work in progress.

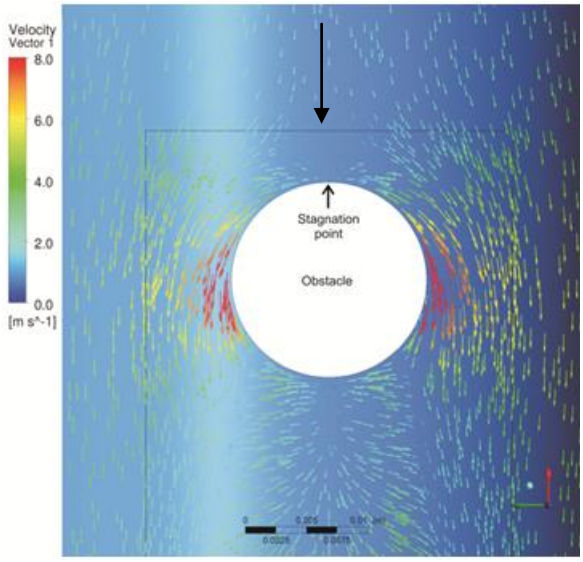

Figure 14. Slurry velocity distribution 0.5 mm from pipe wall surface

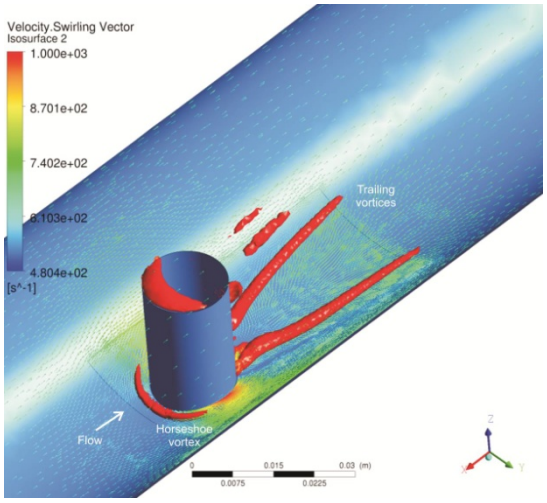

Figure 15. Surface of constant swirl vector equal to 1000 s^{-1}, showing the horseshoe vortex wrapping around the front of the obstacle, and the trailing vortices behind

Figure 16 shows the particle paths from the CFD. The particles decelerate as they approach the stagnation point at the front of the obstacle, then accelerate to greater than 9 m s^{-1} as they pass around it. It is this acceleration that contributes to the substantial erosion scar around the obstacle, since erosion rate is related to particle impact velocity by a power law.

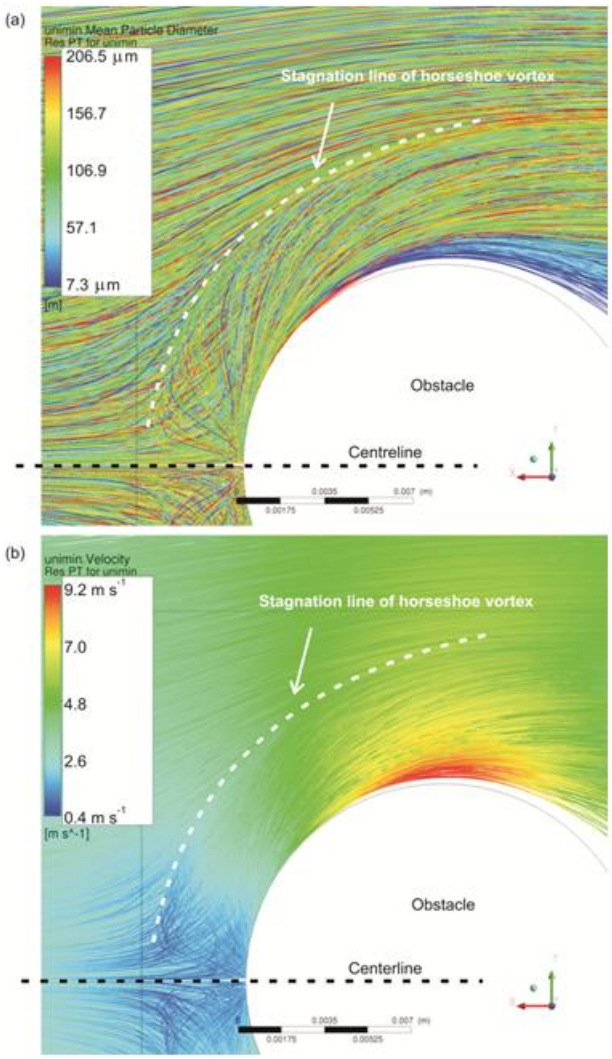

Figure 16. Particle paths hitting and flowing around the obstacle, coloured by (a) particle size, and (b) particle velocity

In terms of reducing the erosion due to the vortex a change must be made to the geometry which reduces the vortex action.

3.2 Surface imperfections

The purpose of this test was to explore another protrusion around a cylinder in pipe sample. In this case, the protrusion was 1.5 mm proud of the test piece and was a cable tie affixed to the cylinder. 316L stainless steel and 27Cr white iron samples were used. 25 µm silica was used as the erodent particles. The superficial velocity was 3.4

m s^{-1}. A photograph of the stainless steel sample before erosion is shown in Figure 17.

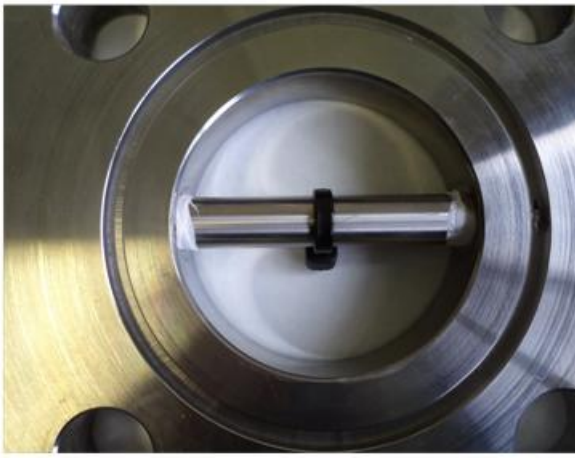

Figure 17 - Cable tie on cylinder in pipe sample, pre erosion

Figure 18 shows the erosion results as measured on the CMM where it can be seen that as for the ductile metals, the white iron also shows increased erosion in the vicinity of the cable tie/cylinder junction. The ratio of the increased erosion to the normal cylinder erosion is 2.8 for this case.

Figure 19 shows the results the 316L cylinder with a cable tie obstacle at 3.4 m s^{-1}. For this case the ratio between the vortex erosion and the cylinder erosion was 3.5 compared with 2.8 for the 27Cr white iron reported above.

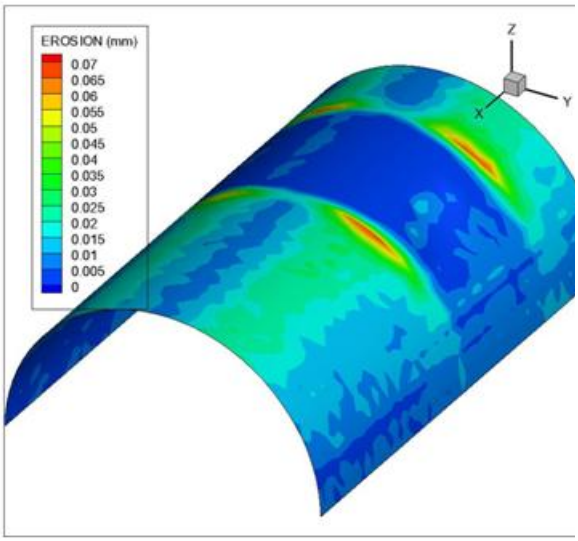

Figure 18. 27Cr white iron erosion with a cable tie obstacle

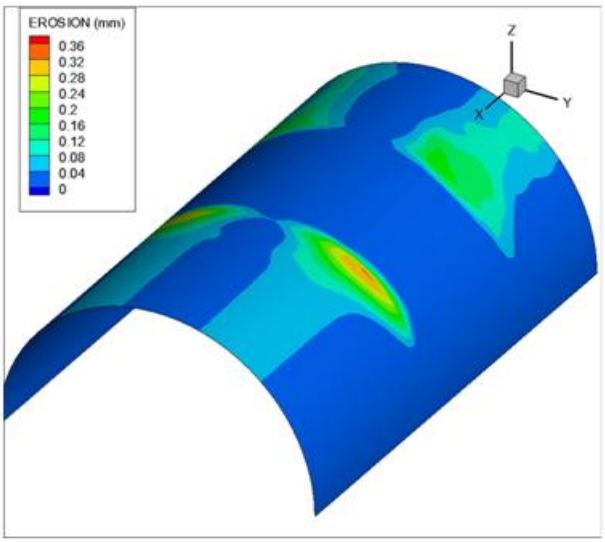

Figure 19. 316L stainless steel at 3.4 m s-1, 209 hours, 100G particles

3.3 Vortex in blanked tee

Figure 20 shows a photograph of an eroded tee blank sample from a test run at 6 m s-1. Figure 21 shows the corresponding CMM measurements. The similarity of these experimental results to the full scale example of Figure 2 is obvious.

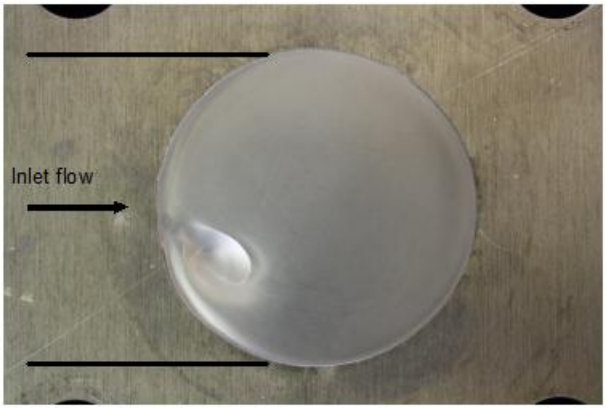

Figure 20. Photograph of sample 48 hours exposure at 6 m s^{-1}

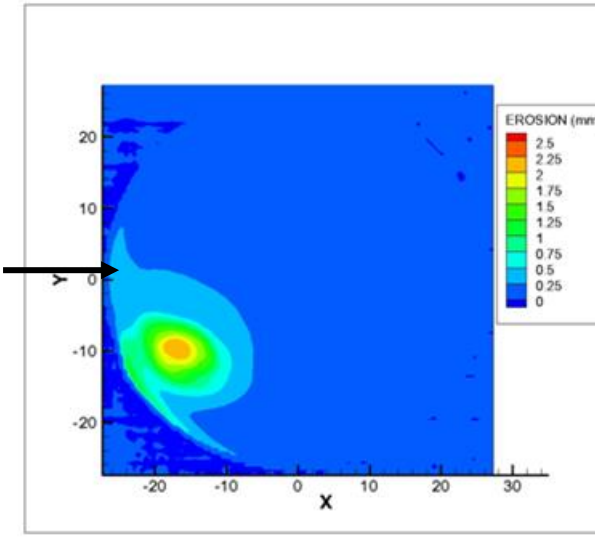

Figure 21. CMM measurements of vortex erosion corresponding to Figure 20

Particles under the action of such a vortex produce more damage than from the direct impact erosion, as confirmed by the measurements that the ratio of such vortex erosion over the reference cylinder is 1.6-3.5 over a variety of tests including aluminium and 316L stainless steel target materials.

It was also observed that erosion occurred on the tee itself in locations near the pipe junction as shown in Figure 22. A photograph of this erosion is shown in Figure 23. Again, reducing or removing the vortex action may reduce this erosion.

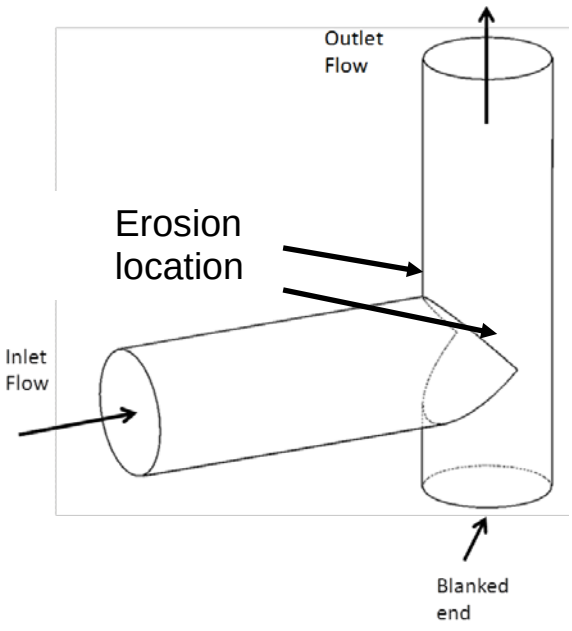

Figure 22. Tee geometry showing location of erosion on the tee itself

Figure 23. Erosion damage on tee. Arrow indicates flow direction

4. CONCLUSION

A variety of flows have been investigated which share the characteristic of a flow disturbance resulting in vortices. These include obstacles on surfaces and a vortex generated in a blanked tee.

Each of these flows shows an increase in erosion relative to that obtained by direct impact which is a consequence of the vortex action. The typical range is 1.6-3.5 times the direct impact erosion as measured on the cylinders used as a reference in each erosion test.

The erosion due to vortex action can also be approximately 80 times the background erosion on a pipe.

The predictability of the vortex in the horseshoe case suggests that it may be useful as a ranking test for material response to erosion under vortex conditions. Current erosion tests, such as the ASTM G65 dry sand rubber wheel, lack any mechanistic connection with the actual mechanism of erosion as experienced under industrial conditions.

A change in the fluid dynamics design of these and other geometries showing vortex flows offers a means of reducing the vortex action and thus providing a reduction in erosion. Tests can be done on model scale systems which can be used to confirm the improved erosion behaviour.

5. REFERENCES

Brown GJ (1999) Erosion prediction in slurry pipeline tee-junctions. In: Second International Conference on CFD in the Minerals and Process Industries, pp. 237-242, Melbourne, Australia: CSIRO

Brown GJ (2002) Erosion prediction in slurry pipeline tee-junctions. Appl Math Model 26:155-170

Graham LJW, Lester DR, Wu J (2010) Quantification of erosion distributions in complex geometries. Wear 268:1066-1071 DOI DOI 10.1016/j.wear.2010.01.011

Simpson RL (2001) Junction flows. Annu Rev Fluid Mech 33:415-443 DOI 10.1146/annurev.fluid.33.1.415

Wu J, Graham LJW, Lester D, Wong CY, Kilpatrick T, Smith S, Nguyen B (2011) An effective modeling tool for studying erosion. Wear 270:598-605 DOI 10.1016/j.wear.2011.01.016

6. ACKNOWLEDGEMENTS

The CSIRO authors are grateful for the support of AMIRA Projects P931 and P931A. Sponsors of these projects are Alcoa, BHPB, Rio Tinto Alcan, Vale and Pentair Valves (Tyco).